SAR IMAGE SEGMENTATION COMBINING THE PM DIFFUSION MODEL AND MRF MODEL

Ganggang Dong[1], *Na Wang*[1], *Canbin* Hu[1,2], *Yongmei Jiang*[1]

[1.] School of Electronic Science and Engineering, National University of Defense Technology, Changsha, P.R. China, 410073

[2.] IETR,UMR CNRS 6164, University of Rennes 1, Rennes, France

ABSTRACT

This paper addresses the statistical segmentation of SAR (Synthetic Aperture Radar) image combining PM (Perona Malik) nonlinear diffusion model and MRF (Markov Random Field) model. First, the original SAR image is filtered using the modified PM nonlinear diffusion model, in which the diffusion coefficients along the tangent direction and the normal direction are approximated and simplified. Afterwards, the filtered image is segmented using MRF model, in which the clique potential is computed using both the label configuration and the intensity information. The proposed method is marked by PM-MRF for short. Experimental results show that PM-MRF competes favorably with the traditional one to segment SAR image homogeneously.

Index Terms— SAR, image segmentation, MRF, PM

1. INTRODUCTION

Speckle, which is inherent in SAR image, makes the traditional segmentation method inefficient, so it is needed to reduce speckle before segmentation. However, many filter algorithms tend to damage the structural detail of the original image when smoothing the noise. As a result, much more isolated errors and distinct misclassification are produced in the segmentation map. PM nonlinear diffusion model [1], based on the scale space, could remove the noise efficiently and preserve the structure of the image meanwhile, but the uniqueness of the solution is not guaranteed, as is widely reported.

MRF model[2][3] is widely used in image processing because it can make full use of the contextual information. Multi-level logistic model [2] (*MLL*) is usually employed to compute the clique potential for its simple form and low computational cost. However, *MLL* model gives the same penalty to the neighbors with different label. As a result, much more misclassification is exhibited in the region boundaries.

In this paper, a new SAR image segmentation method that combines PM nonlinear diffusion model and MRF model is proposed. First, in order to reduce the speckle noise, the original SAR image is filtered using PM diffusion model, in which the diffusion coefficients are simplified using approximate treatment. Second, the filtered image is segmented using the modified MRF model, in which the clique potential is calculated using both the label configuration and the intensity information. Several groups of experimental results demonstrate the better performance of the proposed method than the traditional one.

2. THE METHOD PROPOSED

A. The Description of Image Segmentation

In this paper, the set of sites $S=\{1,2,...,N\}$ is used to index pixels in image plane, and $L=\{1,2,...,M\}$ is the label set that contains discrete labels for the pixels.

Given the observation data $Y=y$, the aim of image segmentation is to accurately estimate the label image $X=x$. The segmentation method using *MAP* criteria is described as $\hat{x}=\arg\max_{x} P(x \mid Y=y)$.

However, it is difficult to directly compute the global posterior probability. In order to make the problem tractable two assumptions should be made. First, the observation data Y are conditionally independent given label image $X=x$. Second, the label of central pixel only depends on the state of its finite neighbors, as Fig. 1 depicted.

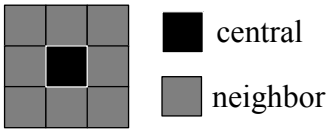

Fig. 1. The neighborhood of 3×3-pixel

From the above assumptions, for any s, which belongs to S, its label is estimated by[4]

$$\hat{x}_s=\arg\max_{x_s} P(y_s \mid x_s)\cdot P(x_s \mid x_N) \qquad (1)$$

where $\hat{x}_s$ denotes the optimum label, and x_N denote the label of the neighbors of x_s.

This algorithm that maximizes the local conditional probability sequentially is called iterated conditional modes (*ICM* [5]). Obviously, *ICM* is a deterministic algorithm, so its convergence is faster than other algorithms. However, the result of *ICM* depends much on the initial segmentation, so it will be insufficient to image which is badly corrupted by noise, because under such circumstances the initial segmentation is coarse. As a result, many misclassification and isolated errors are produced because the algorithm is converged toward the local optimum. This conclusion is demonstrated in the following example, as shown in Fig. 2.

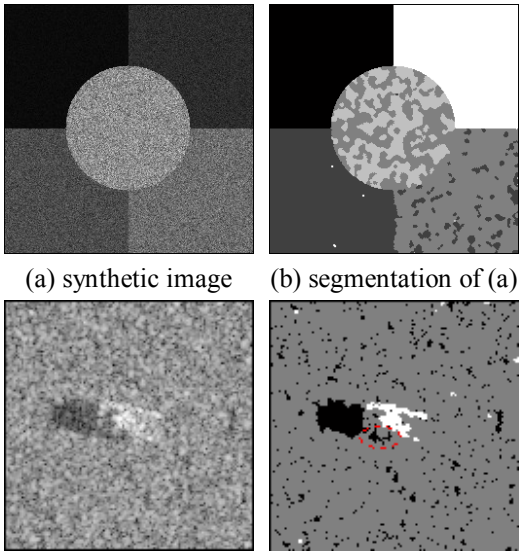

(a) synthetic image (b) segmentation of (a)

(c) real SAR image (d) segmentation of (c)

Fig. 2. Segmentation experiment using ICM

First, a five-class synthetic image of 256×256 pixels in size is built. Each class of the synthetic image has the same grey-level. Then pixels belonging to the same class are multiplied by an exponential noise. The mean of the exponential noise is equal to the grey-level of the class, so the noise grade is strengthened gradually from the left to right and from the top to bottom, and the noise in center circle region of Fig. 2 (a) is the strongest. The purpose of the previous processing is to simulate the formation of speckle in real SAR image. The noisy image is shown in Fig. 2 (a). The segmentation map of Fig. 2 (a) produced using *ICM* is shown in Fig. 2 (b).

Fig. 2 (c) is MSTAR [6] SAR imagery of tank, which have the resolution of one foot both in range and azimuth. The original image is 128×128 pixels in size. The three-class segmentation result of Fig. 2 (c) using *ICM* is demonstrated in Fig. 2 (d).

As can be seen from Fig. 2 (b) and (d), many isolated errors are produced especially in the center circle of Fig. 2 (b) and the background of Fig. 2 (d). This is mainly due to the influence of speckle noise. Moreover, the traditional potential model imposes the same penalty on the neighbors with different labels, in this way, the accuracy of region boundary is lowered badly. Subsequently, PM diffusion model and the intensity-weighted clique potential are employed to solve the problem.

B. The modified PM diffusion model

PM diffusion model is a nonlinear one, with the diffusion law defined by

$$\frac{\partial u(x,t)}{\partial t} = \nabla\left(g(x,t)\bullet\right. \tag{2}$$

where $g(x)$ is the diffusion function, x is the indexes of image plane, and ∇ is the gradient operator. Two forms of diffusion function are presented in paper [1], which is shown as

$$\begin{cases} g(x) = \exp\left(-\dfrac{x^2}{K}\right) \\ g(x) = \dfrac{1}{1+\dfrac{x^2}{K}} \end{cases} \tag{3}$$

where K is the gradient threshold.

Because the solution of PM diffusion model is not unique, as is well-known, some additional clauses are necessary to obtain the uniqueness of the solution. In this paper, approximate treatment is employed to achieve the goal above. First, the diffusion law, as (2) shown, is decomposed along the tangent direction and the normal direction, so (2) is rewritten as

$$\begin{aligned} \frac{\partial u(x,t)}{\partial t} &= \nabla\left[g(|\nabla u|)\bullet\right. \\ &= \Delta u\bullet \quad \bullet \\ &= G(|\nabla u|)\bullet \quad \bullet \end{aligned} \tag{4}$$

where Δ is the Laplace operator; u_{NN} and u_{SS} are the second-order partial differential along the normal direction and the tangent direction; $g(|\nabla u|)$ and $G(|\nabla u|) = g(|\nabla u|) + 2\bullet \quad \bullet$ are the diffusion coefficients along the tangent direction and the normal direction.

Theoretically, the denoising algorithm should remove the noise in the largest while preserve the structural detail of the original image as completely as possible. In this paper, the coefficient along the tangent direction is specified as the unit, and the coefficient along the normal direction is set as $g(|\nabla u|)$, as (5) shown,

$$\frac{\partial u(x,t)}{\partial t} = g(|\nabla u|)\bullet \tag{5}$$

Obviously, the new diffusion law only restricts the diffusion along the normal direction with a factor $f(|\nabla u|)$, and the factor $f(|\nabla u|)$ is the descending function with the argument of the gradient magnitude. On the other hand, the diffusion along the tangent direction is carried out as usual. The performance of the modified PM diffusion model is demonstrated in experiment

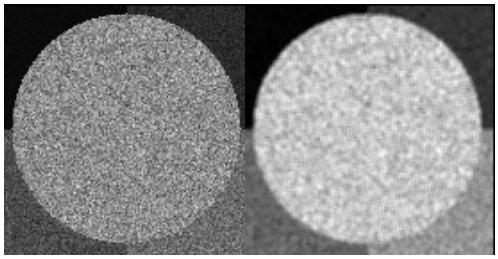

(a) original image (b) result of *Lee* filter

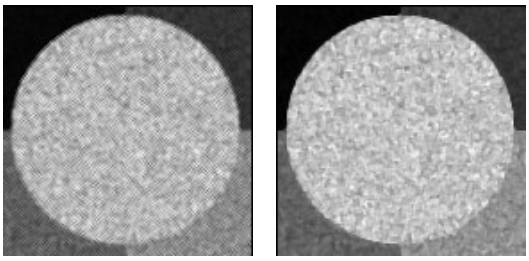

(c) result of *Frost* filter (d) result of *PM* model

Fig. 3.

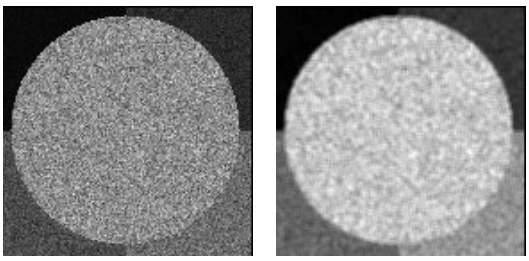

(a) original image (b) result of *Lee* filter

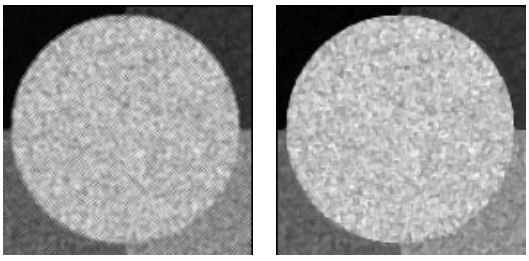

(c) result of *Frost* filter (d) result of *PM* model

Fig. 3. Filter experiment on the simulated SAR image.

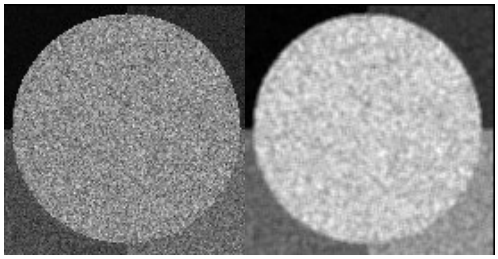

(a) original image (b) result of *Lee* filter

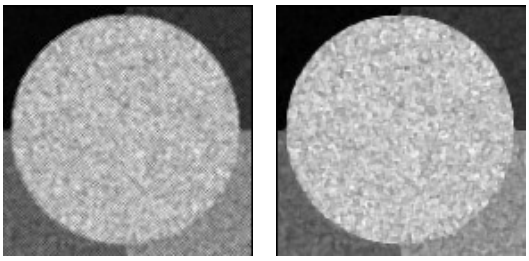

(c) result of *Frost* filter (d) result of *PM* model

Fig. 3 (a) is the center of Fig. 2 (a),

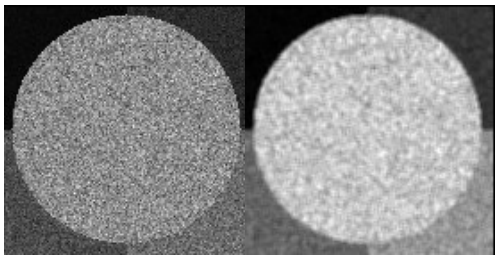

(a) original image (b) result of *Lee* filter

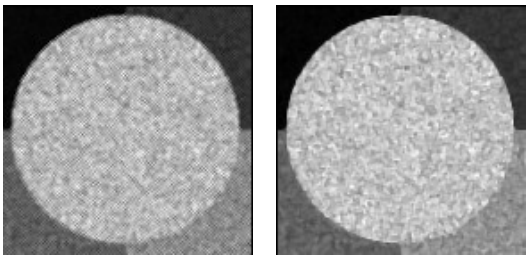

(c) result of *Frost* filter (d) result of *PM* model

Fig. 3 (b), (c) and (d) are the result of *Lee* filter, *Frost* filter and the modified *PM* diffusion model, respectively. It can be seen that the contour of the center circle is blurred by the Lee filter and many spots are produced by the Frost filter. Whereas in Fig. 3 (d), the noise is reduced effectively; and the region contour is preserved well.

C. The intensity-weighted potential function

In *MLL* model, the clique potential only depends on the type of the clique and the local configuration. For cliques that only containing two sites, as is usually employed in image segmentation, the clique potential is defined by

$$V(x_s, x_r) = \begin{cases} \beta & (x_s = x_r) \\ -\beta & (x_s \neq x_r) \end{cases} \tag{6}$$

where x_s is the center element, x_r is the neighbors, and β is the potential parameter.

Obviously, *MLL* model imposes the same penalty on the neighbor elements with different labels regardless of its difference of the intensity. In this way, the contextual information is easily taken into account. However, it is unfavorable to the classification of the region boundary pixels, as is demonstrated in example Fig. 2. Next, the traditional clique potential is modified by introducing the intensity information of the original image. The new cliques function is defined by

$$V(x_s, x_r) = \begin{cases} \beta & (x_s = x_r) \\ -\beta\bullet & (x_s \neq x_r) \end{cases} \tag{7}$$

where $f(d)$ is the weighted coefficient, and $d_{s,r}$ is the intensity distance between x_s and its neighbor x_r.

Theoretically, if x_s is far from x_r, as comparing the intensity value, it is reasonable to postulate that they are belonging to two different classes, so $f(d_{s,r})$ should take on a small value. On the contrary, if x_s is near to x_r, it is much more inclined to believe that they are belonging to the same classes, and $f(d_{s,r})$ should take on a big value similarly. From the discussion above, it seems reasonable to postulate that $f(d_{s,r})$ should be a decreasing function with the argument of the intensity distance. In this paper the following function is proposed

$$f(d_{s,r}) = \exp\left(-\frac{d_{s,r}^2}{K}\right) \tag{8}$$

where K is the gradient threshold, as (3) defined.

As can be seen from (8), the new clique potential is dependent on both the label configuration and the intensity information.

The proposed method is summarized as follows:

1) Reduce the speckle of original image using (5);

2) Segment the filtered image using the MRF model, in which the clique potential is computed using (7).

3. EXPERIMENTAL RESULT

In this section, images presented in Fig. 2 (a) and (c) are segmented again using PM-MRF to assess the segmentation performance of the proposed method.

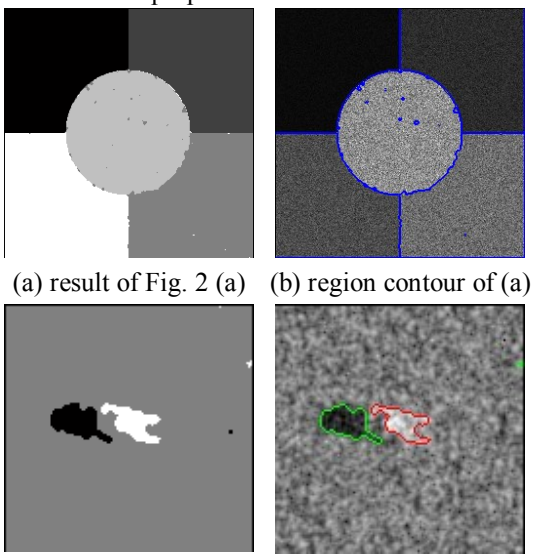

(a) result of Fig. 2 (a) (b) region contour of (a)

(c) result of Fig. 2 (c) (d) region contour of (c)

Fig. 4. Segmentation experiment using PM-MRF.

The original images are detailed in example Fig. 2. The segmentation results obtained using PM-MRF are shown in Fig. 4 (a) and (c), the region contour are shown in Fig. 4 (b) and (d). In Fig. 4 (b), the contour is marked in blue, while in Fig. 4 (d), the contour of the target and the shadow are marked in green and red, respectively.

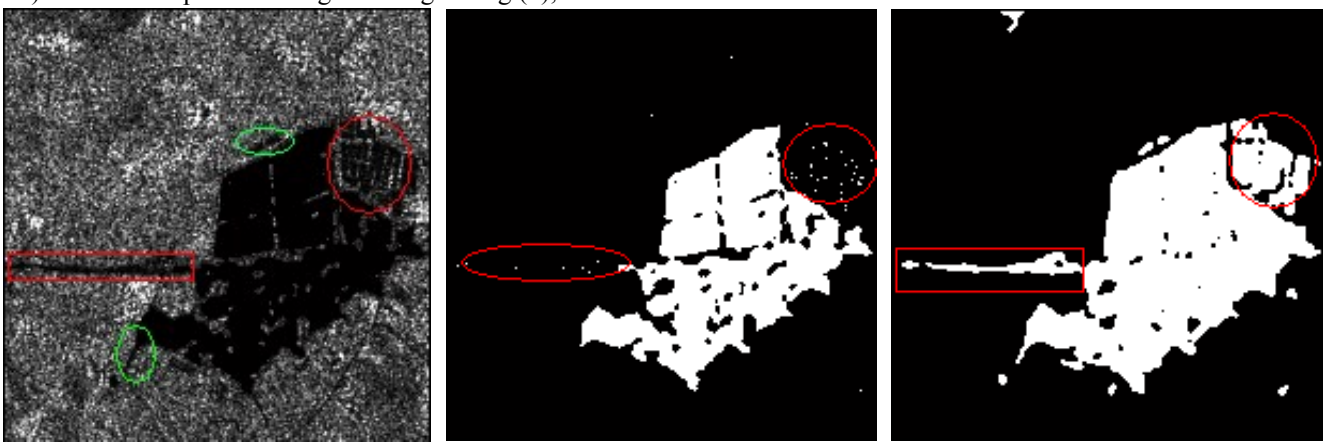

(a) original SAR image (b) segmentation result using *ICM* (c) segmentation result using *PM-MRF*

Fig. 5. Segmentation experiment on SAR imagery of a lake.

As can be seen Fig. 4, the misclassification and isolated errors are eliminated effectively comparing Fig. 2 (b) and (d). The region contour in Fig. 4 (b) and (d) is much more consistent with the original image than the result of *ICM*. Furthermore, the gun barrel of tank in Fig. 2 (c), which is merged into the background clutter thoroughly using ICM, is extracted successfully using PM-MRF.

Subsequently, SAR imagery of a lake is segmented to validate the performance of PM-MRF further. The original image that is 352 × 352 pixels in size is shown in Fig. 5 (a). The results obtained using ICM and PM-MRF are shown in Fig. 5 (b) and (c), respectively.

As can be seen, in Fig. 5 (b), the river located in the west and the northeast corner of the lake (marked in red) are misclassified as the land by ICM, furthermore, the trench located on the north and the southwest (marked in green in Fig4 (a)) are merged into the land. However, all of these misclassification correctly recognized using PM-MRF, as Fig. 5 (c) shown.

4. CONCLUSION

Based on PM diffusion model and MRF model, a new segmentation method for SAR image is proposed in this paper. Firstly, the PM nonlinear diffusion model is modified by simplifying the coefficient along the normal direction and the tangent direction. And then the new diffusion model is used to reduce the speckle noise that is inherent in SAR image. Afterwards, the filtered image is segmented using the modified MRF model, in which the clique potential is computed using both the label value and the intensity information. Several groups of experimental results show that the segmentation result obtained using the proposed method is much more consistent with the original image than *ICM*.

5. REFERENCES

[1] Perona .P, Malik .J, "Scale space and edge detection using anisotropic diffusion". *IEEE Trans. Pattern Anal. Mach. Intell.*, Vol.12, No.7, pp. 629-639. 1990.

[2] Huawu Deng, David A. Clausi, "Unsupervised Image Segmentation Using A Simple MRF Model with A New Implementation Scheme", *ICPR04*, 2004

[3] Samuel Foucher, Mickaël Germain, Jean-Marc Boucher, Goze Bertin Bénié, "Multisource Classification Using ICM and Dempster-Shafer Theory," *IEEE Trans. Instru. Measurement*, Vol.51, NO.2, pp.277-281, April. 2002

[4] Li S.Markov Random Field Modeling In Image Analysis. New York: Springer, 2009:21-34.

[5] Besag. J, "On the statistical analysis of dirty pictures (with discussions)", *Journal of the Royal Statistical Society*, Series B 48, 259-302, 1986.

[6] MSTAR Targets T72 BMP2 BTR70 SLICY(1997). Available:www.mbvlab.wpafb.af.mil /public.